

Analysis of Solar PV Array Fault using Neural Network

Prajakta Pranjan Timane¹, Prof. Y. D. Shahakar²

¹PG Scholar, Electrical Engineering Department, P. R. Pate (Patil) College of Engineering & Management, Amravati

²Assistant Professor, Electrical Engineering Department, P. R. Pate (Patil) College of Engineering & Management, Amravati
Maharashtra, India

Abstract - Solar energy is that the most thick, inexhaustible and clean of all renewable energy resources. Interest in electrical solar PV power generation has accumulated in recent years because of its benefits. This wide distribution of electrical phenomenon panel production wasn't followed by watching, fault detection and designation functions to confirm higher gain.

In this technique, a way for real time watching and fault analysis in electrical solar PV systems is projected. This approach is predicated on a comparison between the performances of a faulty electrical solar PV module, with its correct model by quantifying the precise differential residue which will be related to it. The electrical signature of every default are mounted by considering the deformations induced on the I-V curves and PV curves. All fault cases such as module to module fault, short circuit fault, open circuit fault, cell-ground faults and different shading patterns are considered. The projected technique are often generalized and extended to additional varieties of faults. This faults condition was analyzed by using Back-propagation Based Artificial Neural Network (ANN). The simulation results of MATLAB simulation model shows the satisfied results for different fault condition with variation of solar irradiation.

Key Words: Power Quality Disturbance, Fuzzy logic, Neural Network

1. INTRODUCTION

The solar PV business has big since the oil crises of the Seventies, however has particularly been in fast development in recent years. Per the International Energy Agency (IEA), the planet PV business has developed at average annual rates of V-J Day to twenty from 1991 to 2007 - a growth rate corresponding to that of the semiconductor and laptop industries. Within the recent 10-year amount from 2000 to 2009, world accumulative put in PV power has been increasing from 1,428 MW to 22,893 MW shown in figure 1, with a median annual rate 36.7%, creating it the world's fastest-growing energy technology. The ascent rate is principally because of the necessity for alternatives to fossil fuel-based electricity generation, issues over the world atmosphere, reduced pv prices, and interests in distributed energy sources to boost grid reliableness.

For instance, throughout the past decades, because of the new discovered materials, devices and fabrication strategies, yet as improved solar-cell potency and reliableness, the price of PV has been reduced by many orders of magnitude. Per the International Energy Agency (IEA), PV system prices in according countries has return down from 16 USD per watt in 1991 to 8 USD per watt in 2007.

For succeeding many decades, the PV business has the aptitude to stay a integer annual growth. In a very PV roadmap of IEA, it's calculable that by 2050, the PV power can offer around St Martin's Day of worldwide electricity generation and cut back 2.3 Gigatonnes (Gt) of dioxide emissions per annum. As a number one role in world PV business, the U.S. PV business roadmap contains a semi-permanent goal for 100 percent of U.S. peak electricity generation capability by 2030 is equipped by PV power. It's affordable to predict that the PV business has the potential to play a big role in world electricity generation within the future.

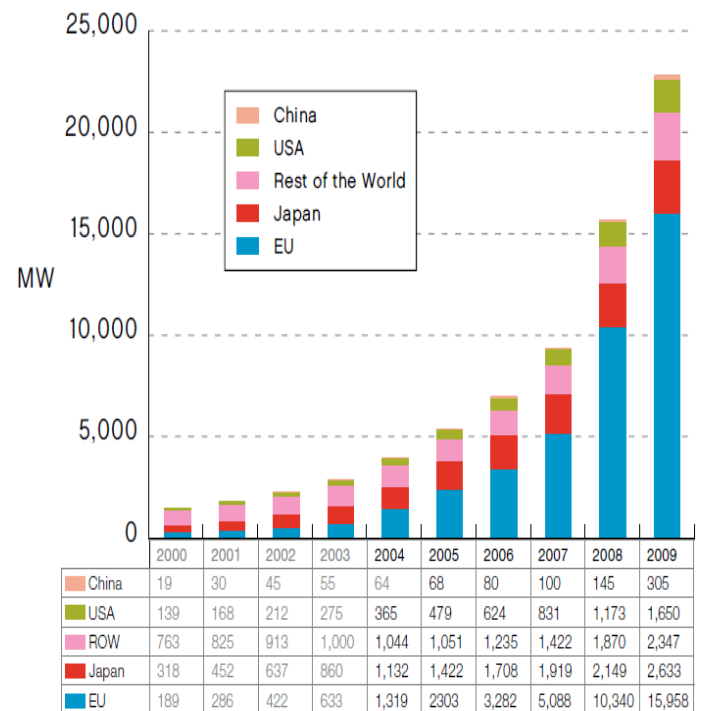


Fig-1: Historical development of world cumulative PV power installed in main Geographies

2. PROPOSED APPROACH

2.1. Block diagram

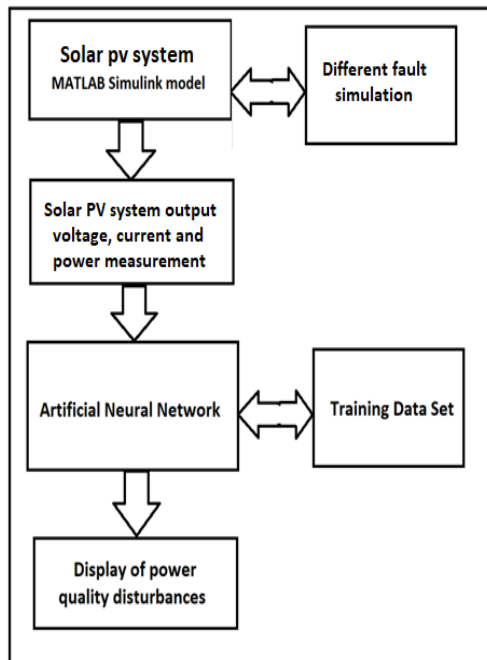


Fig-2: Block diagram of proposed methodology

Figure 2 shows the block diagram of proposed approach in which solar PV module interconnected system design. Then after designing, different fault conditions were simulated using resistance inserted in circuit. The output voltage, current and power were measured at different and that measures parameters were transferred to excel sheet for generation of training data set. That training data set was utilized for training ANN for classification of different pv system fault condition.

3. SIMULATION MODEL

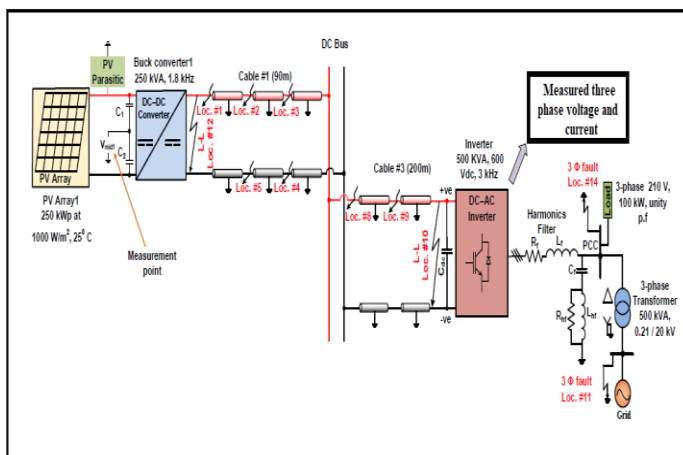


Fig-3: Generalized block diagram of proposed approach

The test system shown in Figure 3 was modeled and simulated in matlab 2015 simulink. A multi-string ungrounded PV system was connected to the grid using a 500 kW, three-phase, 180 degree mode voltage source inverter, which converts DC power generated from the PV array into AC power. One 5 kWp PV arrays was connected to individual DC-DC converters (buck converters) to implement the maximum power point tracking (MPPT) technique. The PV array has 2 parallel strings, and each string consists of 4 modules connected in series. The multi-string PV arrays were connected to a 160 V common DC bus through DC underground cables, and the DC bus was integrated with the DC-link capacitor and the input terminal of the three-phase inverter. The VSI and DC-DC converters were controlled based on the sinusoidal pulse-width modulation (SPWM) technique.

A harmonic filter connects the output terminals of the VSI to respective phases of the point of common coupling (PCC). The 500 kVA, 0.21/20 kV, three phase, Δ/Y , step-up transformer was used to transfer PV power to the distribution system. The station service load was 100 kW, 210 V, unity p.f., three-phase dynamic load that, was connected to the output of the inverter at the PCC. The mid-point voltages (Vmid1 or Vmid2) of the DC-DC converters with respect to grounding were measured and analyzed using a signal processing method for detection and location of faults in the PV system. The PV data are provided in figure 6.5.

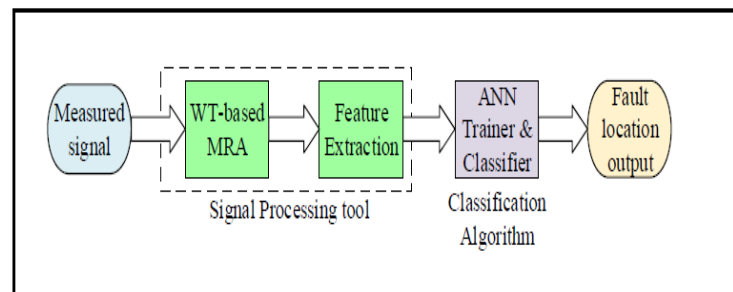


Fig-4: Flowchart of proposed approach

The analysis of high frequency noise patterns to identify fault locations in ungrounded PV systems is proposed. These noise signal patterns are generated due to the power electronic converter switching frequencies and parasitic elements of PV panels and cables (such as cable insulation capacitance and stray inductance). The proposed location method requires a distinguishable signal that uniquely identifies a fault position.

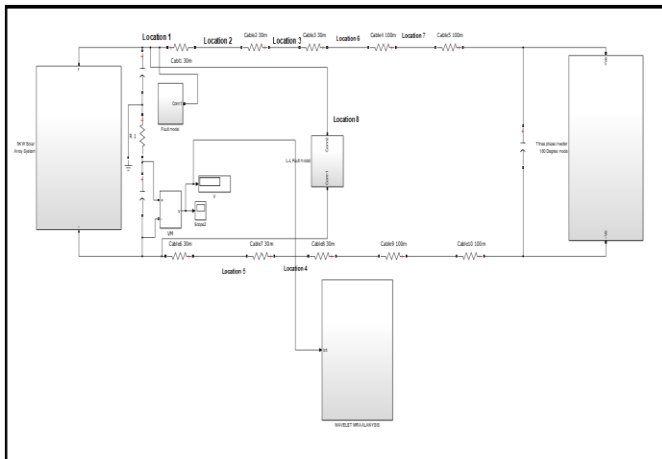


Fig-5: MATLAB simulation of proposed system model

The mid-point voltage of a DC-DC converter 1 (Vmid1) or converter 2 (Vmid2), with measurement points as indicated in Figure 6.1, is monitored. The simulation results illustrate that the high frequency noise is observable in the measured voltage signal and different noise patterns are introduced due to ground faults at various locations of the PV system. Furthermore, the monitored voltage results in a significant change in noise patterns for different ground fault locations. Hence, in this work, the Vmid1 voltage signal is measured and analyzed. No external signal generator is required to locate the fault using the proposed method.

Figure 4 gives a simplistic flowchart of the proposed methodology. The measured time-domain signal is transformed into a time-frequency domain by splitting it into low and high frequency components with a DWT-based MRA technique. The energy or norm of the noise signals at each frequency band gives a unique signature for different fault locations and is used as extracted features for pattern recognition. The extracted features are then used as inputs of a multilayer neural network classification algorithm. The outputs of the ANN classifier give the exact location of the fault.

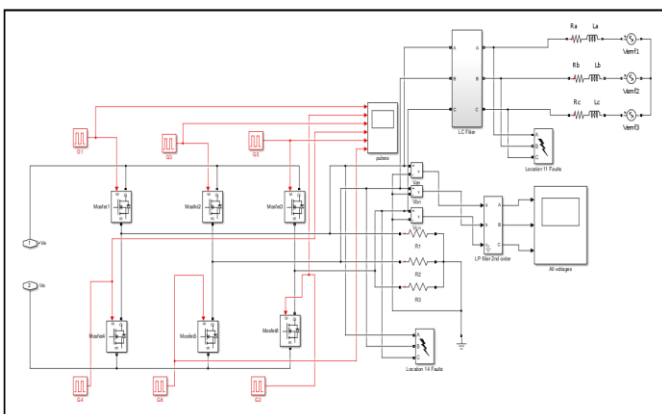


Fig-6: Three phase infinite bus with 180 degree mode inverter subsystem matlab simulink model

Figure 6 shows the complete matlab simulink model implementation of figure 1 in which the matlab model system are divided into three major subsystems. First subsystem model is solar pv array subsystem model in which 5 KW solar pv array system is design the specification of subsystem shown in table 2. Second subsystem model is wavelet multi-resolution analysis subsystem model in which spectral energy and norms features of midpoint output voltage of solar pv array and cable system is analyzed. Third subsystem model is ac grid system in which three phase inverter is design and coupled with three phase 20KV distribution system shown in figure 6.

3.1 Solar PV module design and analysis

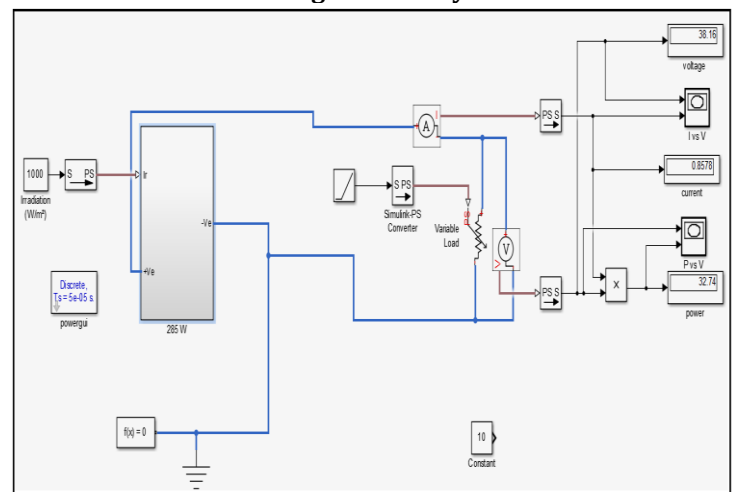


Fig-6: MATLAB Simulation model of 285W PV module system for PV and VI characteristics

Table-1: Solar pv module specification

Electrical Specification	Values
Module efficiency	14.7%
Power output tolerance	+ -3%
Maximum power voltage	35.6 V
Maximum power current	8.02 A
Open circuit voltage Voc	44.7 V
Short circuit current Isc	8.5 A
Peak power Pmax	285 W

Although, there are varies types of solar cell materials, silicon is currently a dominant material utilize in solar cells due to its scalability, momentum and efficiency in light absorption. The fixed PV array has a minimum array size of 5kW. This PV array consists of 4 modules per string connected in series and 4 strings in parallel resulting to 16

modules per array. Each 285W solar panel contains 36 PV cells connected in series as shown in Figure 5 The parameters of the solar module under study are shown in table 1.



Electrical Characteristics

STC	STP285-20/ Wfh	STP280-20/ Wfh	STP275-20/ Wfh
Maximum Power at STC (Pmax)	285 W	280 W	275 W
Optimum Operating Voltage (Vmp)	31.4 V	31.2 V	31.1 V
Optimum Operating Current (Imp)	9.08 A	8.98 A	8.85 A
Open Circuit Voltage (Voc)	38.3 V ±5%	38.1 V ±5%	38.0 V ±5%
Short Circuit Current (Isc)	9.48 A ±5%	9.37 A ±5%	9.24 A ±5%
Module Efficiency	17.2%	16.9%	16.6%
Operating Module Temperature	-40 °C to +85 °C		
Maximum System Voltage	1000 V DC (IEC)		
Maximum Series Fuse Rating	20 A		
Power Tolerance	0/+5 W		

STC: Irradiance 1000 W/m², module temperature 25 °C, AM=1.5; Best in Class AAA solar simulator (IEC 60904-9) used, power measurement uncertainty is within +/- 3%

Fig-7: Electrical Characteristics of 285 W solar PV module (SUNTECH Manufacturer ratings)

Figure 7 shows the name plate of Suntech solar pv 285 W module specification which utilized for system design. Also figure 8 shows the standard manufacturing PV and VI characteristics for suntech 285 W solar pv module for different solar irradiations. As per name plate specification, solar pv module is design in matlab simulink modeling and analysis of module for different solar irradiation is done. Irradiation is varies from 100 W/m² to 1000 W/m² and PV and VI characteristics observed.

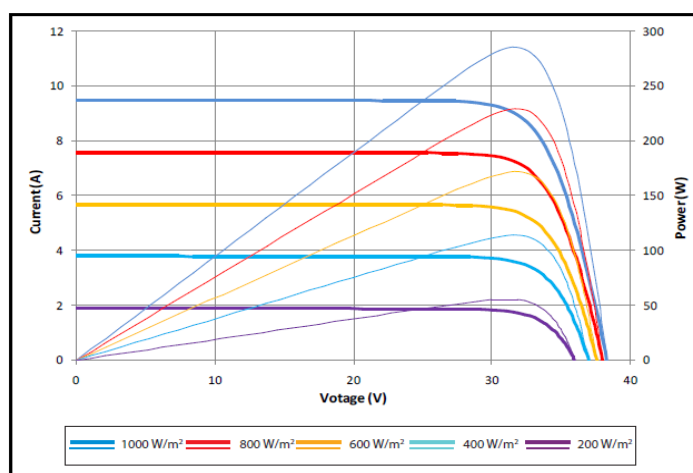


Fig-8: Standard VI and PV characteristics of SUNTECH 285 W solar PV module at different irradiations

3.2 Solar pv module at different irradiation

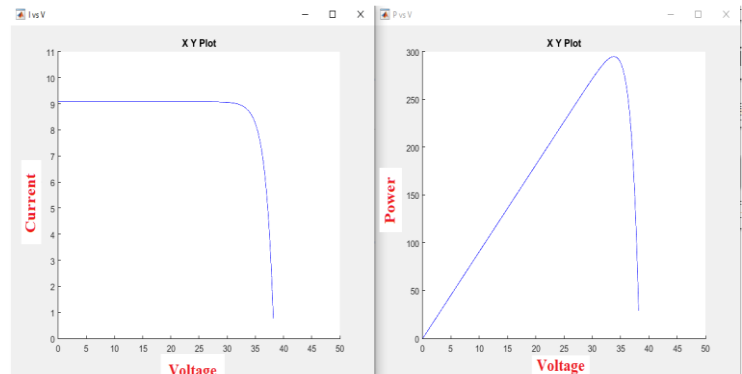


Fig-9: VI and PV characteristics of SUNTECH 285 W solar PV module at 1000 W/m² irradiation using MATLAB simulink modeling

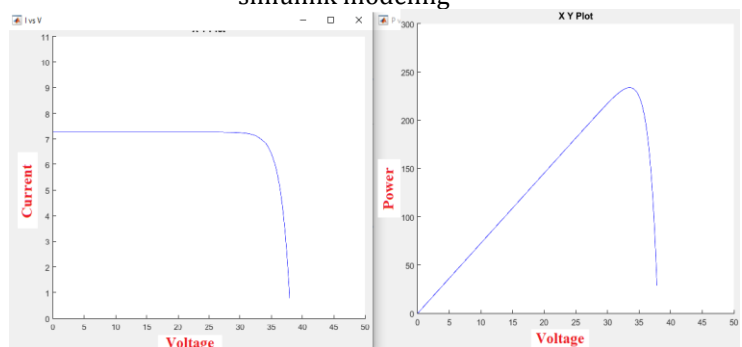


Fig-10: VI and PV characteristics of SUNTECH 285 W solar PV module at 800 W/m² irradiation using MATLAB simulink modeling

3.3 MATLAB Simulink model of 5 KW PV Array subsystem

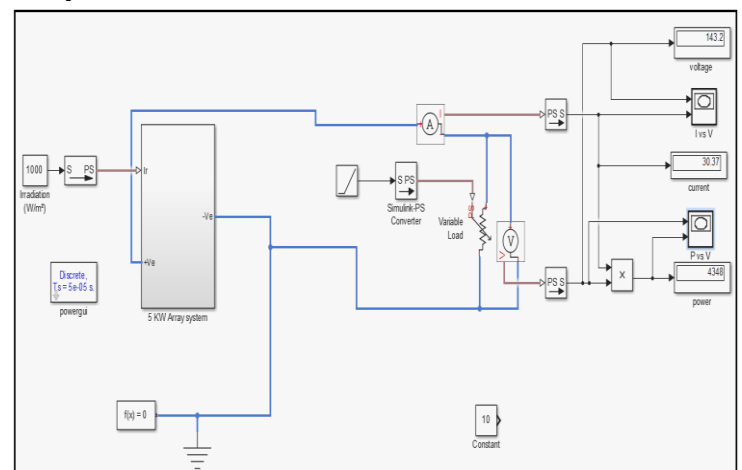


Fig-11: MATLAB simulink model of 5KW solar pv array system for VI and PV characteristics calibration

Figure 11 shows the matlab simulink model for 5KW solar pv module PV-VI characteristics analysis system. In which X-Y plotter used for draw the PV-VI characteristics of KW solar pv array system at different solar irradiation conditions. In this solar array system, there are modules connected in series in one string and 4 parallel string connected for KW

combination generation. The detail specification of complete 5 kw solar pv array system is shown in table 3.

Table-3: Specification of 5KW solar array system

Parameters	Specification
Module manufacture with model code	SUNTECH STP285-20/Wfh
Power output of PV Module	285 W
Module voltage (Voc)	38.3 V
Module short circuit current (Isc)	9.08 A
Number of series connected modules per string	4 Nos
Number of parallel connected strings	4 Nos

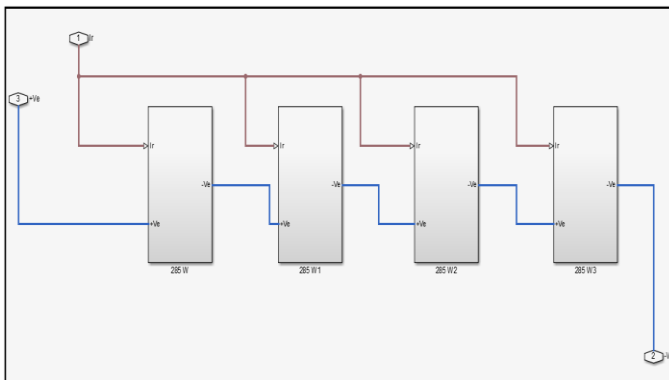


Fig-12: MATLAB simulink model of series connected string-1 subsystem in 5 KW solar array systems

Figure 12 shows the series connected single strings of module in which 4 module of 285 w connected in series manner which generate the open circuit voltage of $V_{oc} = 153$ V and string current i.e. short circuit current of $I_{sc} = 9.08$ A. The total power generated by single string is $P_{max} = 1391.056$ W.

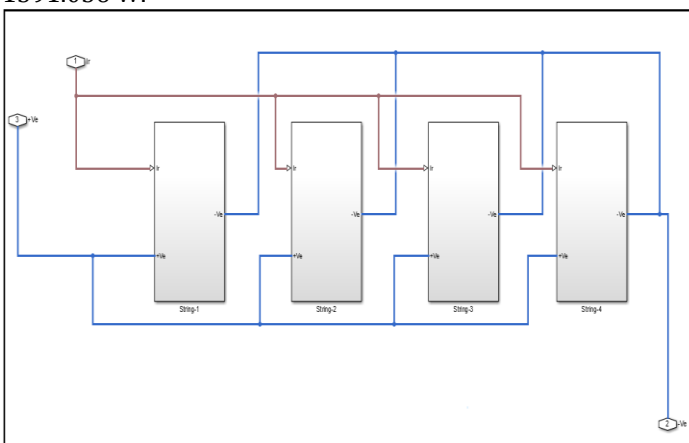


Fig-13: MATLAB simulink model of parallel connected all solar strings subsystem in 5 KW solar array systems
Figure 13 shows the four parallel connected string of solar pv array which generates the total array voltage of $V_{oc} =$

153.2 V and while short circuit current of $I_{sc} = 36.32$ A which generates the maximum power of 5564.224 W which approximately 5 Kw power during normal running conditions.

D. VI and PV characteristics of 5KW solar PV Array system

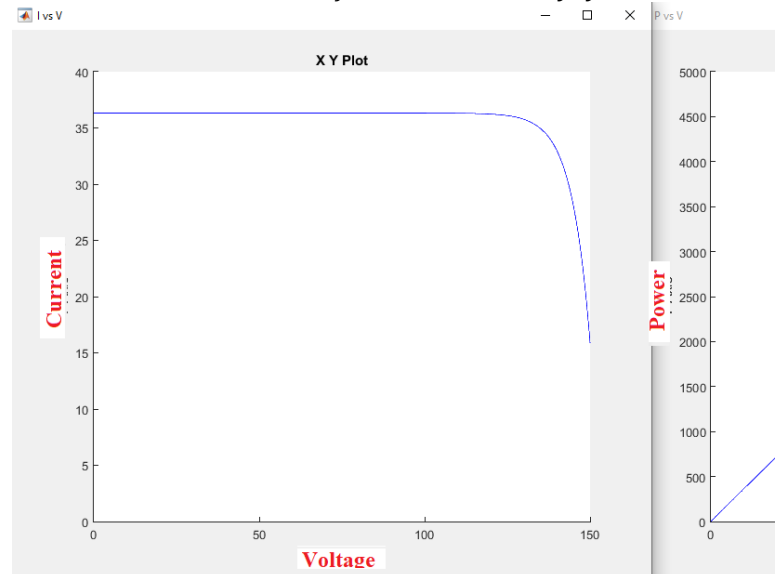


Fig-14: VI and PV characteristics of 5 KW solar PV array at 1000 W/m² irradiation using MATLAB simulink modeling

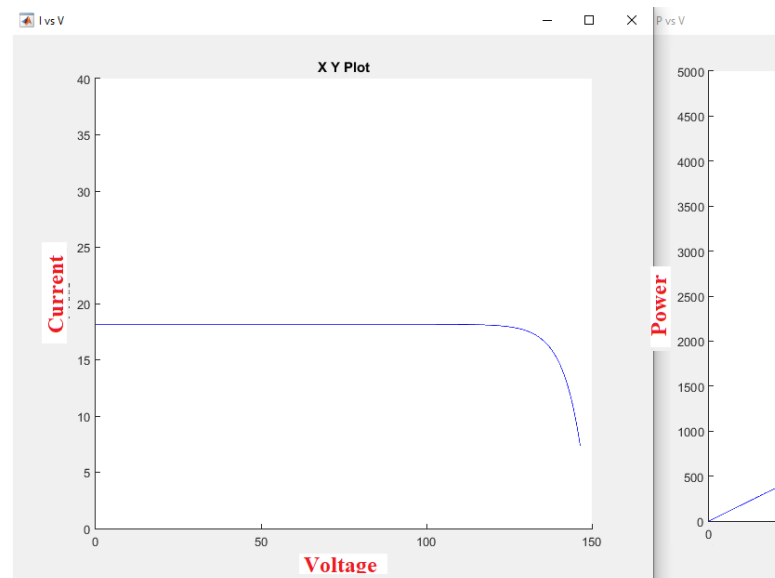


Fig-15: VI and PV characteristics of 5 KW solar PV array at 500 W/m² irradiation using MATLAB simulink modeling

Figure 14 shows the solar pv array 5 kw system PV and VI characteristics at 1000 W/m² standard temperature condition (STC) in which maximum power achieved is 4750 W with open circuit voltage of 150 V and maximum current achieved is 38 Amp. Similarly figure 15 shows the VI and PV characteristics for array system at 500 W/m² in which maximum power achieved is 2250 W and open circuit

voltage is 148 V while short circuit current or maximum current is 17 Amp.

Table 4 shows the solar pv array system measured parameters for different solar irradiation conditions. In which output power, voltage and current are observed. It is clear that as solar irradiation increase then power output of solar array system increases and wise versa.

Sr No	Type of fault	Irradiation (W/m ²)	Voltage (Volts)	Current (Amp)	Power (Watt)
1	Normal	1000	150.2	15.02	2257
2	Normal	800	148	14.8	2191
3	Normal	600	144.3	14.43	2083
4	Normal	400	134	13.4	1794
5	Normal	200	72.64	7.264	527.7
6	Module S12-Gnd	1000	40.38	4.038	163.1
7	Module S12-Gnd	800	39.96	3.996	159.7
8	Module S12-Gnd	500	39.07	3.907	152.6
9	Module S12-Gnd	200	37.04	3.704	137.2
10	Short circuit S33	1000	119.2	11.92	1422
11	Short circuit S33	800	117.7	11.77	1386
12	Short circuit S33	500	113.7	11.37	1294
13	Short circuit	200	72.64	7.264	527.6

	S33				
14	Shading fault S4-23	1000	80.04	8.004	640.6
15	Shading fault S4-23	800	79.16	7.916	626.6
16	Shading fault S4-23	500	77.09	7.709	594.4
17	Shading fault S4-23	200	68.22	6.822	465.4
18	Open circuit String-1	1000	148	14.88	2215
19	Open circuit String-1	800	145.8	14.58	2126
20	Open circuit String-2	500	131.1	13.11	1719

3.4 Three phase AC grid system

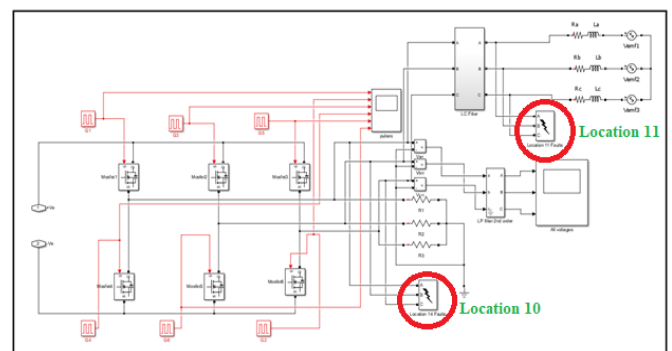


Fig-16: Three phase system with three phase faults in matlab simulink

Figure 16 shows the three phase ac side with three phase faults after inverter at location 10 and at load side in location 11 in which using three phase fault block we have to add three phases faults at each location. Using three phase fault

simulation block we have to simulate LG, LLG, LL and LLL fault in each location.

3.5 ANN Model for solar pv faults analysis

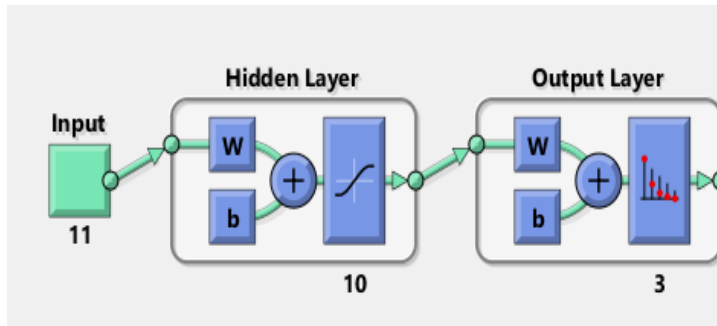


Fig-17: ANN structure for solar pv array fault classification

Figure 17 shows the generalized structure of Artificial Neural Network (ANN) for classification of different solar pv array faults conditions. In which 11 inputs and total three types of faults are used. Inputs are spectral energy of Detail D1 to Detail D10 and Approximation A10 with mother wavelet Symlet used. The output classes are Normal condition, module to ground fault and module to module or short circuit faults classification.

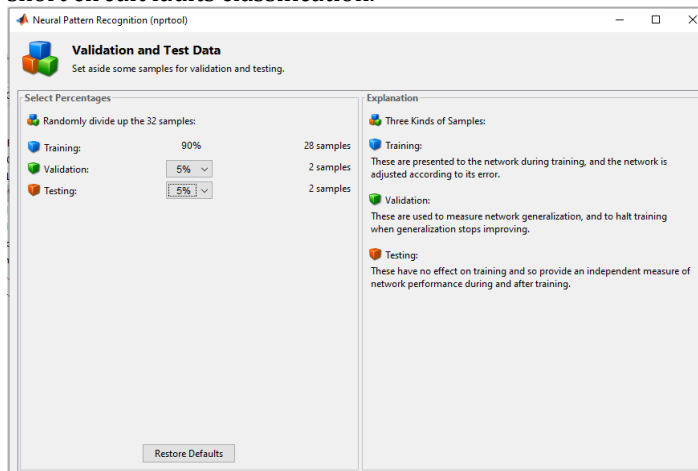


Fig-18: Selection data set window for ANN training for solar pv array fault classification

Table 4 shows the input training data set for ANN for solar pv array fault classification in which there are 32 cases for three types of faults like normal condition, module-ground fault and module-module or short circuit fault. This reading are taken at different solar irradianations. The reading are different mid point voltage, energy of detail signals from D1 to D9 , Energy of approximation signal A9. That data are used for tran the ANN for fault classifications like normal, module-ground and short circuit faults.

Figure 18 shows the selection of percentage of training data set, validation data set and testing data set from entire 32 numbers of training samples.

Training data set: These are presented to the network during training, and the network is adjusted according to its error. This samples are 28 out of 32 samples.

Validation data set: These are used to measure network generalization, and to halt training when generalization stops improving. This samples are 2 out of 32 samples.

Testing data set: These have no effect on training and so provide an independent measure of network performance during and after training. This samples are 2 out of 32 samples.

Figure 19 shows the training performance window for training of pv solar system fault classification neural network. In this total 24 epochs are required for complete training of ANN using back propagation algorithm. Gradient for this training was measures upto as 0.00741.

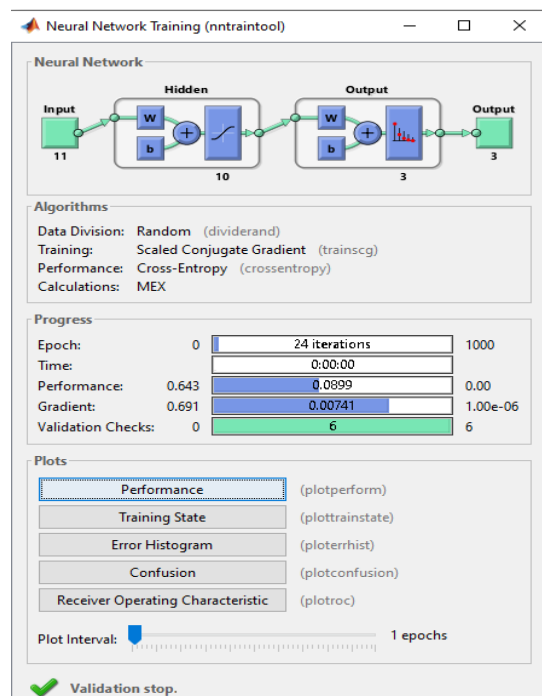


Fig-19: ANN training performance window during training

	Samples	CE	%E
Training:	28	6.18396e-1	10.71428e-0
Validation:	2	3.81090e-0	0
Testing:	2	3.82054e-0	0

Fig-20: ANN results after training for solar pv array fault classification

Figure 20 shows, for training of ANN, total 32 data sample was utilized out of which 28 data set i.e. 70% data utilized for training. For validation and testing 30% dataset was utilize i.e. 4 sample data set. Also MSE (Mean square error) for all data set was 10.71 % after successful training of ANN.

3.6 ANN Results



Fig-21: Confusion matrix of ANN for solar pv array fault classification

Figure 20 shows that 90.6 % data are perfectly classify the different pv solar system fault cases and 10 % data not classify properly i.e. ANN confused for classification. It means that for remaining 10 % data set neural network was in confusion state for classify the fault. Perfectly classify all types of solar pv array fault classes in table 4.

Figure 21 shows the receiver operating characteristic is a metric used to check the quality of classifiers. For each class of a classifier, roc applies threshold values across the interval [0,1] to outputs. For each threshold, two values are calculated, the True Positive Ratio (the number of outputs greater or equal to the threshold, divided by the number of one targets), and the False Positive Ratio (the number of outputs less than the threshold, divided by the number of zero targets).

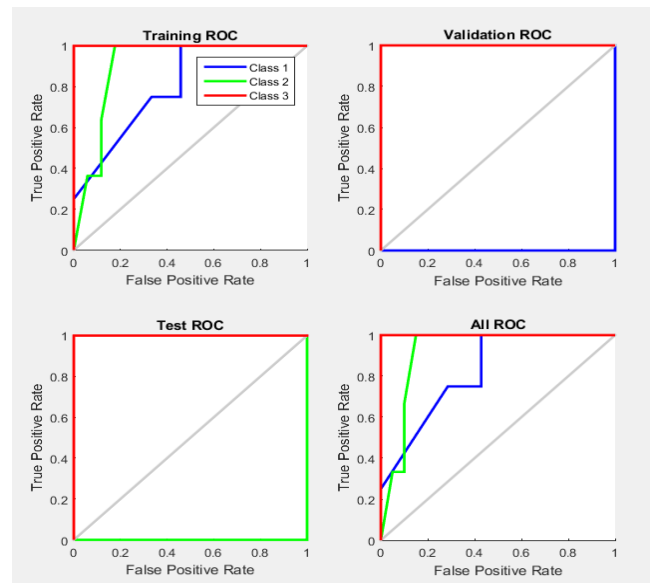


Fig-22: Receiver operating characteristics (ROC) of ANN for solar pv array faults classification

4. CONCLUSION

A fault location scheme for ungrounded PV systems has been presented. The ungrounded PV system was subjected to various faults (line to ground, line-line and arc faults) on both the DC and AC sides of the system. The DWT-based MRA technique was studied to extract the unique features of the noise signal measured at the mid-point of the DC-DC converter. Then, a three-layer feed-forward ANN and back propagation based were adopted as a classifier of the pattern recognition to identify exact fault locations for the cables and PV modules of the ungrounded PV systems. Compared to existing methods in the literature, the proposed method does not require an external high frequency signal injector, reduces the number of voltage sensors, and can locate the fault while the system remains operational. Finally, the results show the proposed method is promising, accurate, and robust with respect to changes in operating parameter values and with noisy inputs.

REFERENCES

[1] Dhar, Snehamoy, Rajesh Kumar Patnaik, and P. K. Dash. "Fault detection and location of photovoltaic based DC microgrid using differential protection strategy." IEEE Transactions on Smart Grid 9.5 (2017): 4303-4312.

[2] Schirone, L., et al. "Fault finding in a 1 MW photovoltaic plant by reflectometry." Proceedings of 1994 IEEE 1st World Conference on Photovoltaic Energy Conversion-WCPEC (A Joint Conference of PVSC, PVSEC and PSEC). Vol. 1. IEEE, 1994.

[3] Karatepe, Engin, and Takashi Hiyama. "Controlling of artificial neural network for fault diagnosis of photovoltaic array." 2011 16th International Conference on Intelligent System Applications to Power Systems. IEEE, 2011.

[4] Jiang, Lian Lian, and Douglas L. Maskell. "Automatic fault detection and diagnosis for photovoltaic systems using combined artificial neural network and analytical based methods." 2015 International Joint Conference on Neural Networks (IJCNN). IEEE, 2015.

[5] Pan, Yan, Michael Steurer, and Thomas L. Baldwin. "Ground fault location testing of a noise pattern based approach on an ungrounded DC system." 2010 IEEE Industrial and Commercial Power Systems Technical Conference-Conference Record. IEEE, 2010.

[6] Uyar, Murat, Selcuk Yildirim, and Muhsin Tunay Gencoglu. "An effective wavelet-based feature extraction method for classification of power quality disturbance signals." *Electric power systems Research* 78.10 (2008): 1747-1755.

[7] Prasanth Ram, J., Rajasekar, N., 2017. A new global maximum power point tracking technique for solar photovoltaic (PV) system under partial shading conditions (PSC). *Energy* 118, 512–525.

[8] Miyatake, M., Veerachary, M., Toriumi, F., Fujii, N., Ko, H., 2011. Maximum power point tracking of multiple photovoltaic arrays: a PSO approach. *IEEE Trans. Aerosp. Electron. Syst.* 47 (1), 367–380.

[9] Lin, Xue, Wang, Yanzhi, Pedram, M., Kim, Jaemin, Chang, Naehyuck, 2014. Designing fault-tolerant photovoltaic systems. *IEEE Des. Test* 31 (3), 76–84.

[10] Villalva, M.G., Gazoli, J.R., Filho, E.R., 2009. Comprehensive approach to modeling and simulation of photovoltaic arrays. *IEEE Trans. Power Electron.* 24 (5), 1198–1208.

[11] Hung T. Nguyen, Nadipuram R. Prasad, Carol L. Walker and Elbert A. Walker, "A First Course In Fuzzy and Neural Control", A CRC Press Company, Boca Raton London New York Washington, D.C.